

Design of geocell reinforcement for supporting embankments on soft ground

G. Madhavi Latha*

Department of Civil Engineering, Indian Institute of Science, Bangalore - 560 012, India

(Received September 17, 2010, Accepted May 19, 2011)

Abstract. The methods of design available for geocell-supported embankments are very few. Two of the earlier methods are considered in this paper and a third method is proposed and compared with them. In the first method called slip line method, plastic bearing failure of the soil was assumed and the additional resistance due to geocell layer is calculated using a non-symmetric slip line field in the soft foundation soil. In the second method based on slope stability analysis, general-purpose slope stability program was used to design the geocell mattress of required strength for embankment. In the third method proposed in this paper, geocell reinforcement is designed based on the plane strain finite element analysis of embankments. The geocell layer is modelled as an equivalent composite layer with modified strength and stiffness values. The strength and dimensions of geocell layer is estimated for the required bearing capacity or permissible deformations. These three design methods are compared through a design example. It is observed that the design method based on finite element simulations is most comprehensive because it addresses the issue of permissible deformations and also gives complete stress, deformation and strain behaviour of the embankment under given loading conditions.

Keywords: geocell; reinforcement; embankment; soft ground; design; composite model; finite element analysis.

1. Introduction

Construction of embankments over weak soils is a commonly encountered problem in many geotechnical applications like highway and airport runway embankments, containment dikes, flood protection levees, earth dams and berms. Among various stabilization techniques available for embankments on soft soils, providing high strength geosynthetic reinforcement at the base of the embankment is simple, faster and cost-effective. Use of geocells for reinforcing the embankments over weak soils has gained lot of popularity in recent years. Geocells are three-dimensional form of geosynthetic materials with interconnected cells filled with soil or aggregate. The important advantages of geocell layer at the base of the embankment are:

- It acts as an immediate working platform for the construction.
- It acts as a stiff rigid base to the embankment, promoting uniform settlements.
- It minimizes construction time and eliminates excavation and replacement costs.

*Corresponding author, Associate Professor, E-mail: madhavi@civil.iisc.ernet.in

- It prevents bearing capacity failure and minimizes excessive settlements and lateral deformations.
- It provides short and long term global stability to the embankment.

Very few investigations are reported in literature on the performance of geocell reinforced earth structures by Bathurst and Jarrett (1988), Jenner *et al.* (1988), Bush *et al.* (1990), Dean and Lothian (1990), Bathurst and Karpurapu (1993), Cowland and Wong (1993), Bathurst and Knight (1998), Hendricker *et al.* (1998), Krishnaswamy *et al.* (2000), Madhavi Latha and Rajagopal (2007), Madhavi Latha *et al.* (2008) etc. The methods of design available for geocell-supported embankments are very few. In this paper, a new design method based on the finite element analysis of geocell supported embankments is proposed for designing the geocell reinforcement and this method is compared with two of the earlier methods.

2. Existing design methods

Very few researchers have explored the methods for designing geocells. Some of them are given by Puig and Schaffner (1986), Wu and Austin (1992) and Rimoldi and Ricciuti (1994). But these methods are for designing geocells along the slope for erosion control applications. As per the knowledge of the author, there are only two methods available in literature for designing geocell reinforcement to support embankments on soft clay foundation. The first method is the slip line method proposed by Jenner *et al.* (1988). The second method is based on slope stability analysis, proposed by Madhavi Latha *et al.* (2006).

2.1 Slip line method

Jenner *et al.* (1988) suggested a method for designing geocells for supporting embankments. In this design, plastic bearing failure of the soil was assumed instead of slip circle failure. This type of failure was expected for embankments, whose width is more than four times the depth of the foundation soil. The methodology developed by Johnson and Mellor (1983) for the compression of a block between two rough, rigid plates was used for determining the bearing capacity of the soft foundation soil. The soft soil, which was analogous to the block, was assumed to get compressed between the geocell mattress at the top and the hard stratum at the bottom. This analogy was used for developing a non-symmetric slip line field in the soft foundation soil. The concept of this design is that the geocell mattress exerts a degree of restraining influence on the deformation mechanism of the soft soil, thus rotating the direction of principal stresses. The direction of maximum shear stress also rotates correspondingly, pushing the failure surface deep into the foundation soil. A 15° slip line field was used to determine the bearing resistance of the soft soil. The construction of slip line field and corresponding bearing pressure diagram are discussed in detail by Jenner *et al.* (1988). Typical bearing capacity diagram for the geocell supported embankment drawn based on the slip line field is shown in Fig. 1.

The bearing capacity diagram was developed by working from the outer edge of the slip line field inwards to the boundary of the 'rigid head', defined on the slip line field by the ratio of geocell width to the depth of the soft layer. The 'rigid head' is the term used by Jenner (1988) to denote the soil zone, which does not experience plastic strains. Thus the slip line field is used to define the maximum allowable pressure distribution within a zone of limiting plasticity.

where σ_n = vertical stress on the element.

$$x = \frac{2\sigma_n \sin^2 \phi' \pm [4\sigma_n^2 \sin^4 \phi' - 4(\sin^2 \phi' - 1)(\sigma_n^2 \sin^2 \phi' - \tau^2)]^{1/2}}{2[\sin^2 \phi' - 1]} \quad (3)$$

t = shear stress at the interface (C_u in limiting condition)

f = friction angle for the geocell fill material

The rotation of principal stress occurs within the mattress depth. Therefore a geocell mattress having tensile strength equal to the expected horizontal stress should be used to support the embankment.

2.2 Design based on slope stability analysis

The design of reinforcement for embankments based on slope stability analysis is developed by Madhavi Latha *et al.* (2006). This method uses a general-purpose slope stability program to design the geocell mattress of required strength for embankment. The computer program developed for conducting slope stability analysis of geocell supported embankments takes the slope geometry, height of geocell layer, depth of foundation soil, shear strength parameters of embankment soil and geocell layer, properties of foundation soil, pore pressure co-efficient and the value of uniform surcharge pressure on the crest as input parameters. The program uses Bishop's method of slices for calculating the factor of safety. The program automatically searches for different trial slip circles and gives the lowest factor of safety and coordinates of the center of the critical slip circle. The reliability of the computer program was ensured by running some example problems. Factor of safety obtained from the program for these problems was in agreement with the lowest factor of safety obtained from graphical method by drawing several trial slip circles and obtaining the factor of safety for each of these circles using conventional method of slices.

For designing the geocell mattress below an embankment, geocell layer is treated as a layer of soil with cohesive strength greater than the encased soil and angle of internal friction same as the encased soil. This is because; geocells provide all-round confinement to the soil due to the membrane stresses in the walls of geocells, because of which apparent cohesion is developed in the soil. Using the rubber membrane theory proposed by Henkel and Gilbert (1952), Bathurst and Karpurapu (1993) analyzed the cohesive strength of soil encased in a single geocell in triaxial compression. The same analysis was extended for multiple geocells and also for geocells made of geogrids by Rajagopal *et al.* (1999), Madhavi Latha (2000) and Madhavi Latha and Murthy (2007).

The additional confining pressure due to the membrane stresses can be written as (Henkel and Gilbert 1952)

$$\Delta\sigma_3 = \frac{2M\varepsilon_c}{D} \frac{1}{(1-\varepsilon_a)} = \frac{2M}{D_o} \left[\frac{1-\sqrt{1-\varepsilon_a}}{1-\varepsilon_a} \right] \quad (4)$$

where ε_a = axial strain at failure

ε_c = circumferential strain at failure

D_o = initial diameter of sample

D = diameter of the sample at an axial strain of ε_a

M = modulus of the membrane

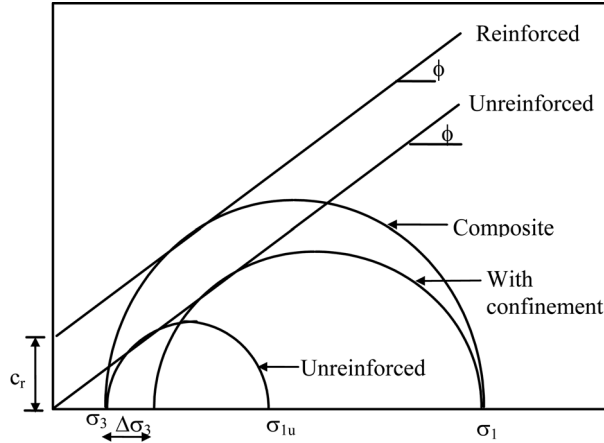


Fig. 2 Mohr circles for calculating the strength improvement due to geocell reinforcement

The above equation was used to calculate the additional confining pressure due to geocell reinforcement, using the parameters as follows. D_o was taken as the initial diameter of geocell. The geocell pockets are not circular but are triangular in shape. The equivalent diameter for the triangular shaped geocells can be obtained by equating the area of the triangle to a circle of equivalent area. M is the modulus of the geocell material at axial strain ϵ_a , determined from the load-strain curves obtained from wide width tensile strength test on geogrids.

The relation between the induced apparent cohesive strength and the additional confining stress due to the geocell can be derived by drawing Mohr circles for the unreinforced and reinforced soil samples as shown in Fig. 2. The additional cohesive strength due to geocell layer can be obtained as (Rajagopal *et al.* 1999)

$$c_r = \frac{\Delta\sigma_3}{2} \sqrt{k_p} \tag{5}$$

Substituting the value of $\Delta\sigma_3$ obtained from Eq. (4) in Eq. (5), we will get the apparent cohesion induced to soil due to geocell confinement. This additional cohesive strength is added to the original cohesive strength of soil encased in geocells to get the cohesive strength of geocell layer (c_g).

For preliminary design problems, if the geometry of the embankment, properties of foundation and embankment soils are given, we can perform slope stability analysis with trial values of height of geocell layer and determine the cohesive strength of geocell layer required to get a design value of factor of safety. From this cohesive strength, we can back calculate the modulus of geocell required for assumed values of pocket-size of geocell and axial strain in the walls of geocell.

This design method has been verified for the case of geocell supported model embankments constructed in laboratory with varying pocket sizes of cells, varying height of geocell mattress, for geocell layers made of different geogrids and for sand and clay infill materials by Madhavi Latha *et al.* (2006). It was observed that the maximum surcharge pressure at which the embankments failed in the model tests was agreeing well with the surcharge pressure at which the factor of safety was obtained as one in the slope stability analysis.

2.3 Proposed design based on finite element analysis

Using finite element technique for the stability analysis of reinforced earth embankments was attempted earlier by researchers like Roy *et al.* (2009). Based on the laboratory experiments, Madhavi Latha (2000) proposed an equivalent composite model for geocell encased sand. Later Rajagopal *et al.* (2001) validated the equivalent composite model using experiments on geocell supported model embankments constructed over soft clay bed. In this model, the induced cohesion in the soil is related to the increase in the confining pressure on the soil due to the geocell reinforcement through Eq. (5) given in the previous section. The equivalent stiffness of geocell encased soil is related to the stiffness of unreinforced soil, secant modulus of geocell material and interaction parameter, which represents the interaction in case of multiple cells. Based on triaxial compression tests on geocell encased sand, Madhavi Latha (2000) and Rajagopal *et al.* (2001) proposed the following nonlinear empirical equation to express the Young's modulus of geocell-reinforced sand (E_g) in terms of the secant modulus of the geocell material and the Young's modulus parameter of the unreinforced sand (K_u).

$$E_g = P_a [K_u + 200M^{0.16}] \left(\frac{\sigma_3}{P_a} \right)^{0.7} \quad (6)$$

In which P_a = atmospheric pressure

M = secant modulus of geocell material in kN/m

σ_3 = confining pressure

The modulus parameter in the above equation corresponds to the modulus number in hyperbolic model proposed by Duncan and Chang (1970). The main advantage of the Eq. (6) is that for any given geocell material, the equivalent modulus number can be obtained by simply substituting the value of the modulus (M). This value of M should be corresponding to the average strain of 2.5% in the tensile load-strain response of the geogrids. The circumferential strain in geocells, at the center of the geocell mattress, when the footing settled typically about 30 to 35% of footing width, was found to be of the order of 2.5% from the earlier research of the author (Madhavi Latha *et al.* 2008). This strain value is considered as the average circumferential strain in the geocells, while estimating the increase in the confining pressure on the soil due to geocell encasement.

To design a geocell supported embankment, the embankment should be simulated in a finite element program. The geocell layer of trial dimensions can be simulated using the composite model with equivalent strength and stiffness as discussed in earlier sections. Pressure-settlement response of the embankment will give the bearing capacity of the embankment and the corresponding settlement below the embankment, heave of the ground surface adjacent to the embankment and also the lateral deformations of the slope. By comparing the response against the specified design requirements, the dimensions and strength of geocell layer can be altered to get the desired bearing capacity within permissible deformations. The advantage of the finite element based design method is that complete contours of the stresses and deformations in the embankment as well as in the foundation soil could be obtained, which is not possible in the other two design methods described.

To verify the validity of the finite element model used for the design, laboratory model tests on geocell supported embankments constructed on soft clay foundation described by Krishnaswamy *et al.* (2000) are simulated using the finite element model and the results are compared. Schematic diagram of this embankment with the properties of foundation clay and embankment soil are shown

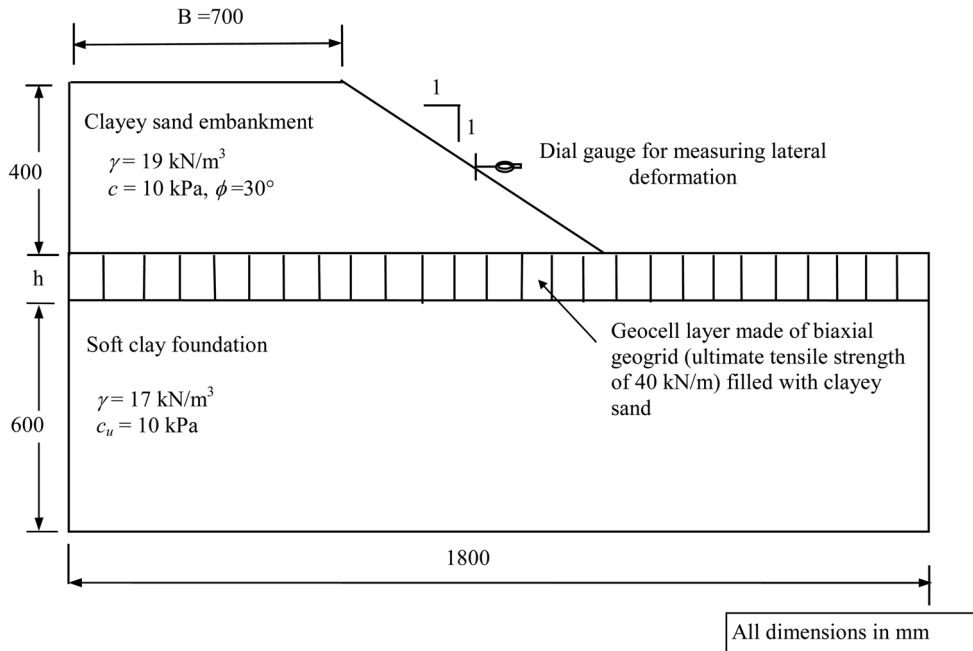


Fig. 3 Laboratory model of geocell supported embankment (After Krishnaswamy *et al.* 2000)

in Fig. 3. The finite element analyses are performed using the finite element program GEOFEM (Karpurapu and Bathurst 1993). Comparison of the lateral deformations of the slope for different aspect ratios of the geocells is presented in Fig. 4. Aspect ratio for geocells is defined as the ratio of height (h) to equivalent diameter (D) of the cells. As the geocell pockets are triangular in shape,

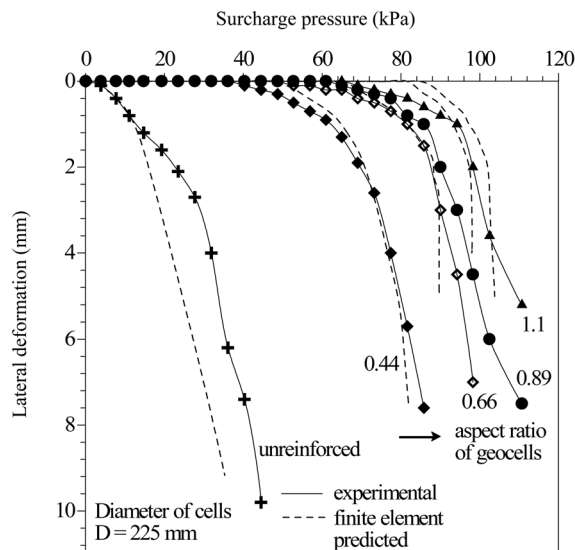


Fig. 4 Comparison of response of laboratory model embankments supported on geocells with different aspect ratios (D/h)

equivalent diameter is obtained by equating the area of the triangle to a circle of equivalent area. In these model tests, the diameter of the cells is kept constant as 225 mm and the height of the geocell layer is varied to obtain different aspect ratios of the cells. Lateral deformations are chosen for comparison because the model tests are conducted in a steel test tank and hence the settlements are influenced by the hard tank base, whereas the embankment is free to move in lateral direction. These results establish that the composite finite element model is able to capture the response of the geocell supported embankments well and could be used in the design with confidence.

3. Design example

It is proposed to construct a 6 m high embankment over 6 m thick layer of soft cohesive soil with undrained shear strength of 15 kN/m². The cross section of embankment is shown in Fig. 5. A surcharge of 20 kN/m² will be applied. Design suitable geocell mattress for this case.

3.1 Design based on slip lines

Embankment base width = 66 m

Width of geocell mattress = 66 m – 4 m (leaving 2 m offset either side) = 62 m

Width of geocell/depth of soft soil layer = 62/6 = 10.33

From stress field diagram, $P/c_u = 12$ (obtained from the stress field diagram as explained by Jenner *et al.* 1988 and Bush *et al.* 1990)

Average pressure across rigid head $P' = 12 c_u + c_u = 13 C_u$

Hence the bearing capacity diagram for the symmetric half of the embankment can be drawn as shown in Fig. 6.

Load from half of the embankment allowing a surcharge pressure of 20 kN/m² is calculated as follows:

Load from the weight of the embankment above the geocell layer (crest width 18 m, base width 28 m and height 4 m) = $(18+28)/2 \times 4 \times 19 = 1748$ kN/m

Load from the weight of the portion of the embankment where geocell is inserted (base width 33 m, and height 2 m) = $33 \times 2 \times 19 = 1254$ kN/m

Load from surcharge on the crest (18 m long) = $18 \times 20 = 360$ kN/m

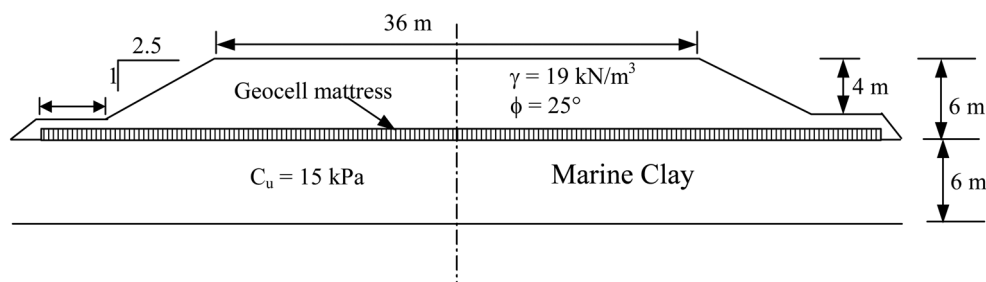


Fig. 5 Cross section of the embankment in design example

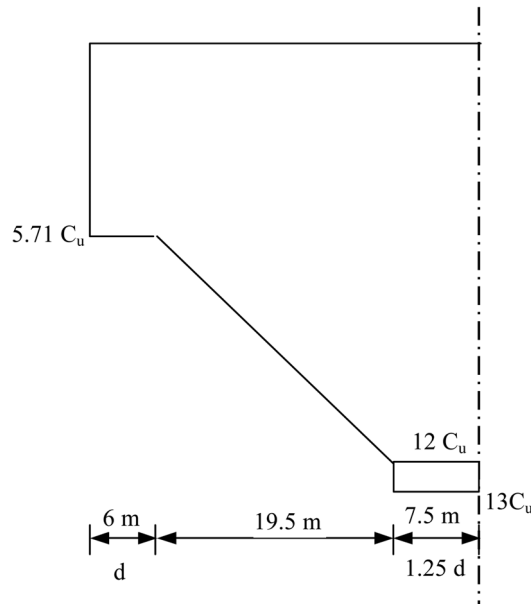


Fig. 6 Bearing capacity diagram for the design example

Total load from half of the embankment, including the surcharge = $1748 + 1254 + 360 = 3362$ kN/m

Bearing capacity in kN/m for the half of the embankment from the pressure diagram:

$$6 \times 5.71 c_u + (5.71 + 12)/2 \times c_u \times 5.71 + 7.5 \times 13 c_u = 304.43 c_u$$

$$c_u \text{ required for equilibrium} = 3362/304.43 = 11.04 \text{ kN/m}^2$$

$$\text{Actual } c_u = 15 \text{ kN/m}^2$$

Factor of safety against bearing capacity failure = $15/11.04 = 1.35$ (against 1.25 required). Hence safe.

For designing the geocell mattress, consider an element of soil within the granular cellular mattress, but interfacing with the soft layer. The stress condition in element can be obtained from a Mohr-circle construction as shown by Jenner *et al.* (1988).

$$\text{The horizontal stress on the element: } \sigma_h = \sigma_n - 2 x$$

$$\tau = \text{shear stress at the interface} = c_u \text{ in limiting condition} = 11.04 \text{ kN/m}^2$$

$$\sigma_n \text{ under highest part of the embankment} = 6 \times 19 + 20 = 134 \text{ kN/m}^2$$

$$\phi = 40^\circ \text{ for the geocell fill material (preferable soil fill)}$$

$$x \text{ calculated as per Eq. (3)} = 51.36 \text{ kN/m}^2$$

$$\sigma_h = \sigma_n - 2 x = 134 - 2 \times 51.36 = 31.28 \text{ kN/m}^2$$

The rotation of principal stress occurs within the mattress depth. Therefore mattress strength required = 31.28 kN/m. Hence a geocell mattress of 1 m height with long term tensile strength more than 31.28 kN/m should be used to support the embankment, with a geogrid base. The strength of the bottom geogrid layer is not considered in the design. This basal geogrid gives additional factor of safety by increasing the stiffness of the geocell layer and lateral restraintment to

the soft soil layer, apart from facilitating the installation of geocell layer.

3.2 Design based on slope stability analysis

From slope stability analysis of unreinforced embankment shown in Fig. 5, the minimum factor of safety is obtained as 0.83. The failure slip circle from the slope stability analysis of unreinforced embankment is shown in Fig. 7.

$\phi = 40^\circ$ for the geocell fill material (preferable soil fill)

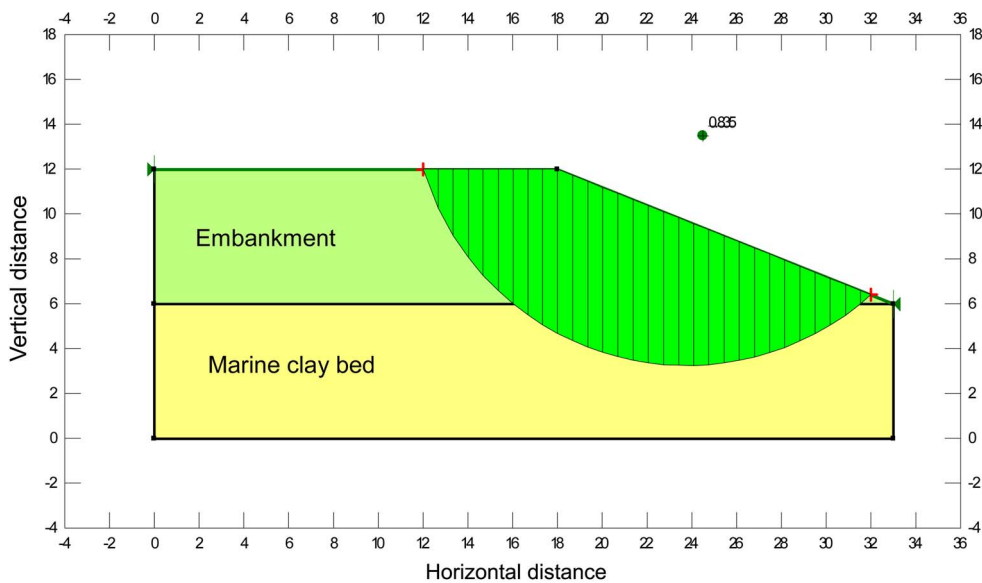


Fig. 7 Design example: slope stability analysis of unreinforced embankment

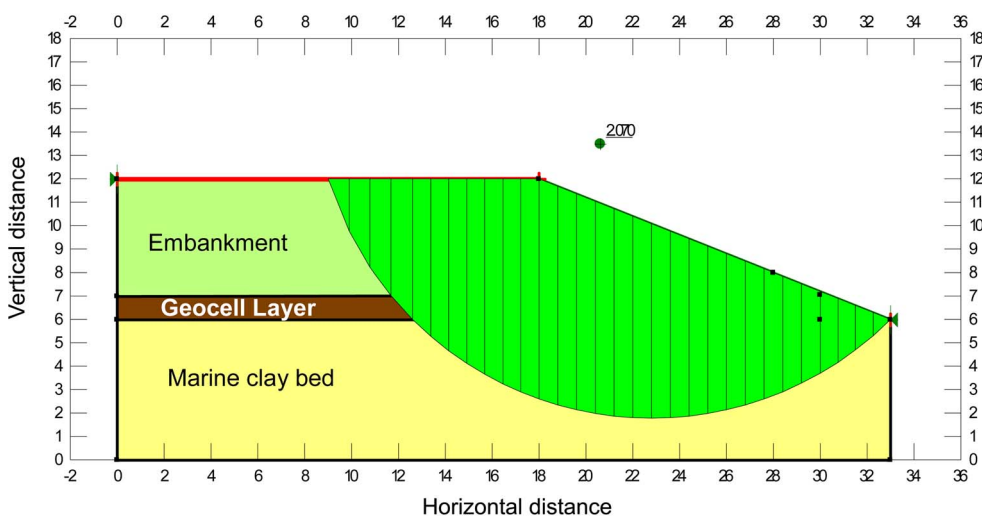


Fig. 8 Design example: slope stability analysis of geocell supported embankment

Height of geocell layer = 1 m

Geocell layer will have angle of internal friction of 40°

By conducting slope stability analysis with trial values of cohesion of geocell layer, for a desired factor of safety of 2.0, the cohesive strength of geocell layer (c_g) is obtained as 28 kPa. The failure slip circle from the slope stability analysis of the geocell supported embankment is shown in Fig. 8.

As the fill soil is cohesionless, additional cohesive strength to be derived from geocell reinforcement (c_r) is 28 kPa. For a ϕ value of 40° , k_p is 4.59. Substituting the values of c_r and k_p as 0 and 4.59 in Eq. (7), $\Delta\sigma_3$ is obtained as 26 kPa.

Diameter of geocells is assumed as 1 m to get an aspect ratio (h/D_0) of 1. Substituting the values of $\Delta\sigma_3$, D_0 and taking axial strain in geocell walls as 2.5% in Eq. (4), M is obtained as 1000 kN/m. Thus a geocell layer of 1 m height and pocket size of 1 m with geocells made of geogrids having secant modulus at 2.5% strain (M) as 1000 kN/m could be provided at the base of the given embankment. Biaxial geogrids with ultimate tensile strength of about 40 kN/m normally fall in this range (Murali Krishna and Madhavi Latha 2007).

3.3 Design based on finite element analysis

The embankment shown in Fig. 5 is simulated in finite element analysis as discussed in the proposed method in earlier sections in the finite element program GEOFEM. The geocell layer was modeled as an equivalent composite layer just like any soil layer. This modeling approach is reasonably good in simulating both the stiffness and strength of geocell encased soils. The interfaces between the soft clay foundation and geocell layer and also between the embankment fill and the geocell layer were modeled using 4-noded zero thickness interface elements described by Goodman *et al.* (1968) considering a zero thickness continuous element in which strains were computed from relative nodal displacements. The finite element meshes were generated with nodes on either side of the interface, which are connected through joint elements. The shear stiffness of these elements was initially defined as very high (106 kPa/m) to ensure the compatibility of displacements of nodes on either side of the interface. The shear stiffness of interfaces between the soil and reinforcement was modelled using stick-slip type formulation in which perfect bond was assumed when the shear stress is less than the shear strength defined by the Mohr-Coulomb model. Once the shear stress reaches the shear strength of the interface (τ_f), the shear stiffness is reduced to a small value that is 1000 times less than the initial value to allow for relative movement between the reinforcement and soil. The normal stiffness was kept constant at a high value (106 kPa/m) throughout the analysis to ensure the continuity of the nodes in the vertical direction. The tensile normal stresses were not allowed to develop in these elements.

The constitutive behaviour of the soft foundation soil and the soil in the embankment was simulated using Mohr-Coulomb elastic-perfectly plastic yield surface with a non-associated flow rule. The average Young's modulus (E) and Poisson's ratio (μ) for the foundation soil are taken as 1 MPa and 0.45 which are reasonable values for the undrained cohesive strength value of 15 kPa (US Army Corps of Engineers 1990, EM 1110-1-1904). These values are taken as 60 MPa and 0.3 for the embankment fill. For the geocell layer, the Young's modulus value is calculated using Eq. (6) for any trial value of M , taking the confining pressure as the minor principal stress acting at the centerline of the geocell layer. Modulus number for the geocell fill soil is taken as 1000, which is selected from Janbu (1963) for medium-coarse sand. The settlement response of the embankment

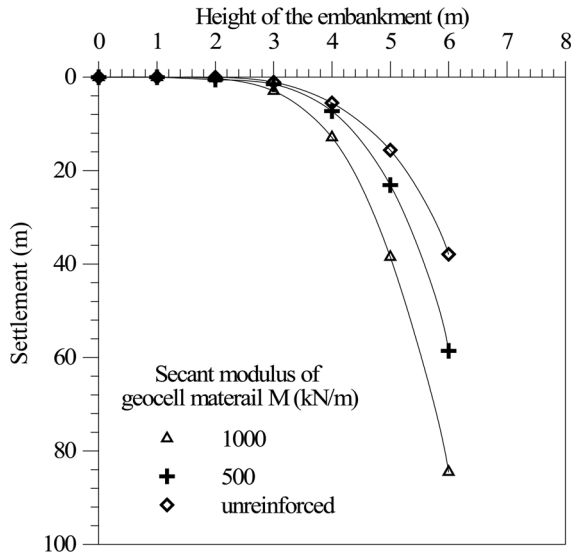


Fig. 9 Settlement below the embankment in design example

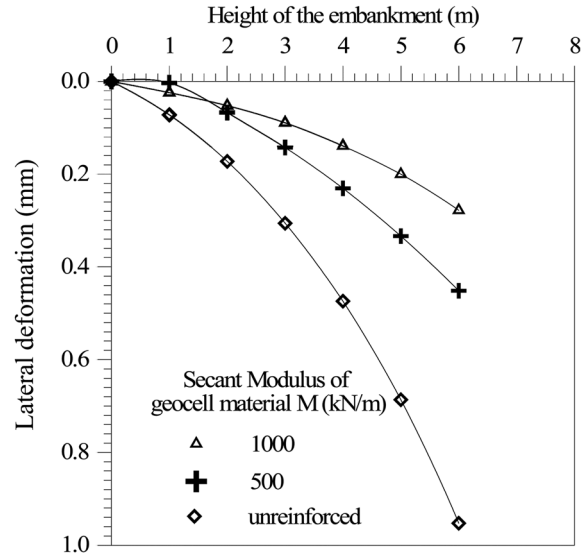


Fig. 10 Lateral deformation near the toe in design example

with geocells of secant modulus values of 500 kN/m and 1000 kN/m along with unreinforced embankment are shown in Fig. 9. The lateral deformations near the toe are shown in Fig. 10.

As observed from the Fig. 9, unreinforced embankment settled by about 1 m at the end of construction. When the embankment is supported on a layer of geocells of secant modulus (at 2.5% strain) of 500 kN/m, the settlement reduced to 0.46 m. When the secant modulus of geocell material is increased to 1000 kN/m, the settlement at the end of construction is reduced to 0.28 m, which is less than 5% of the total height of the embankment. This is taken as the ultimate limit state settlement as per the guidelines given by US Army Corps of Engineers (UFGS-35 73 13, 2008). Hence it is recommended to provide a geocell layer of 1 m height just above the soft foundation soil using a geosynthetic material of secant modulus more than or equal to 1000 kN/m to control the settlements below the embankment to permissible levels due to increase in surcharge pressure during the construction of embankment.

As observed in Fig. 10, the geocell layer with secant modulus of 1000 kN/m is effective in substantially reducing the lateral deformations near the toe. As mentioned in the previous section, this modulus value corresponds to commercially available biaxial geogrids with ultimate tensile strength of about 40 kN/m.

4. Discussion

As illustrated through the design example, all the three methods discussed in the paper have ultimately suggested similar geocell reinforcement for the given embankment. However, each method has its own advantages and limitations. The method based on slip lines is very complicated compared to the other two methods, as it needs construction of slip line field for every embankment problem and calculation of bearing capacity across the rigid head. The second method based on the

slope stability analysis is the simplest of the three because, it just needs performing slope stability check in any standard program by replacing the geocell layer with a layer of soil whose properties are arrived at based on the geocell dimensions and material used. The third method based on the finite element simulations is the most comprehensive of all because it deals with complete simulation of the embankment. The deformations, stresses and shear strains in the embankment at any location can be obtained in this method. Also, the method includes design based on permissible settlements at given embankment height, which is not addressed in the other two methods. The limitation of this method is that the finite element simulations need accurate evaluation of properties of soil and geocell material through laboratory experiments. Regarding the accuracy of the results, all three methods are giving almost same range of design output with certain assumptions made in the finite element analyses. Slip line method and slope stability analysis can be used for preliminary design and the same can be verified by finite element studies, where complete deformation analysis and shear strain contour generation is possible.

5. Conclusions

A new method for the design of geocell supported embankments based on finite element simulations is proposed in this paper. This method is compared with the two existing methods; slip line method and slope stability method. A design example of embankment over soft soil is worked out using all three methods and the relative advantages and limitations of each method are brought out. All three methods are giving almost similar results. Slip line method is very complicated compared to other two methods. Slope stability method makes lot of simplifications and is based on the factor of safety against slope failure, which may not be critical. The design method based on finite element simulations is most comprehensive because it addresses the issue of permissible deformations and also gives complete stress, deformation and strain behaviour of the embankment under given loading conditions. It is suggested that the slip line and slope stability methods should be used for preliminary designs and the same need to be verified by the method based on finite element simulations.

References

- Bathurst, R.J. and Jarrett, P.M. (1988), "Large-scale model tests of geo-composite mattresses over peat subgrades", *Transportation Research Record 1188*, Transportation Research Board. Washington, D.C., 28-36.
- Bathurst, R.J and Karpurapu, R. (1993), "Large-scale triaxial compression testing of geocell-reinforced granular soils", *Geotech. Test. J.*, **16**(3), 296-303.
- Bathurst, R.J. and Knight, M.A. (1998), "Analysis of geocell reinforced soil covers over large span conduits", *Comput. Geotech.*, **22**, 205-219.
- Bush, D.I., Jenner, C.G and Bassett, R.H. (1990), "The design and construction of geocell foundation mattress supporting embankments over soft ground", *Geotext. Geomembranes*, **9**, 83-98.
- Cowland, J.W. and Wong, S.C.K. (1993), "Performance of a road embankment on soft clay supported on a geocell mattress foundation", *Geotext. Geomembranes*, **12**, 687-705.
- Dean, R. and Lothian, E. (1990), "Embankment construction problems over deep variable soft deposits using a geocell mattress", *Proceedings of Performance of Reinforced Soil Structures*, British Geotechnical Society, London (UK), 443-447.
- Roy, D., Chiranjeevi, K., Singh, R. and Baidya, D.K. (2009), "Rainfall induced instability of mechanically

- stabilized earth embankments”, *Geomech. Eng.*, **1**, 193-204.
- Duncan, J.M. and Chang, C.Y. (1970), “Non-linear analysis of stresses and strains in soils”, *J. Soil Mech. Found. Div.*, **96**(5), 1629-1653.
- Goodman, R.E., Taylor, R.L. and Brekke, T.L. (1968), “A model for the mechanics of jointed rock”, *J. Soil Mech. Found. Div.*, **94**, 637-659.
- Hendricker, A.T., Fredianelli, K.H., Kavazanjian, Jr. E. and McKelvey, III J.A. (1998), “Reinforcement requirements at a hazardous waste site”, *Proceedings of 6th International Conference on Geosynthetics*, Atlanta (USA), 465-468.
- Henkel, D.J. and Gilbert, G.C. (1952), “The effect of rubber membranes on the measured triaxial compression strength of clay samples”, *Geotechnique*, **3**, 20-29.
- Janbu, N. (1963), “Soil compressibility as determined by oedometer and triaxial tests”, *Proceedings of VI European Conference on SMFE*, Wiesbaden, pp 19-25.
- Jenner, C.G., Bush, D.I. and Bassett, R.H. (1988), “The use of slip line fields to assess the improvement in bearing capacity of soft ground given by a cellular foundation mattress installed at the base of an embankment”, *Proc. Int. Geotech. Symp. Theory and Practice of Earth Reinforcement*, Balkema, Rotterdam (The Netherlands), 209-214.
- Johnson, W. and Mellor, P.B. (1983), *Engineering plasticity*, Ellis Marwood Ltd., Chichester (UK).
- Karpurapu, R. and Bathurst R.J. (1993), *Users’ manual for geotechnical finite element modelling GEOFEM*, Vol.1-3, Department of Civil Engineering, Royal Military College, Kingston, Ontario (Canada).
- Krishnaswamy, N.R., Rajagopal, K. and Madhavi Latha, G. (2000), “Model studies on geocell supported embankments constructed over soft clay foundation”, *Geotech. Test. J.*, **23**, 45-54.
- Madhavi Latha, G. (2000), “Investigations on the behaviour of geocell supported embankments”, Ph.D. thesis, Indian Institute of Technology Madras, Chennai, India.
- Madhavi Latha, G. and Murthy, V.S. (2007), “Effects of reinforcement form on the behaviour of geosynthetic reinforced sand”, *Geotext. Geomembranes*, **25**, 23-32.
- Madhavi Latha, G. and Rajagopal, K. (2007), “Parametric finite element analyses of geocell supported embankments”, *Can. Geotech. J.*, **44**(8), 917-927.
- Madhavi Latha, G., Dash, S.K. and Rajagopal, K. (2008), “Equivalent continuum simulations of geocell reinforced sand beds supporting strip footings”, *Geotech. Geol. Eng.*, **26**(4), 387-398.
- Madhavi Latha G., Rajagopal, K. and Krishnaswamy, N.R. (2006), “Experimental and theoretical investigations on geocell supported embankments”, *Int. J. Geomechanics*, **6**(1), 30-35.
- Murali Krishna, A. and Madhavi Latha, G. (2007), “Seismic response of wrap-faced reinforced soil retaining wall models using shaking table tests”, *Geosynth. Int.*, **14**(6), 355-364.
- Puig, J. and Schaeffner, M. (1986), “The use of three dimensional geotextile to combat rainwater erosion”, *Proc. of Third International Conference on Geotextiles*, Vienna, Austria, Vol. **IV**, 1137-1142.
- Rajagopal, K., Krishnaswamy, N.R. and Madhavi Latha, G. (1999), “Behavior of sand confined in single and multiple geocells”, *Geotext. Geomembranes*, **17**, 171-184.
- Rajagopal, K., Krishnaswamy, N.R. and Madhavi Latha, G. (2001), “Finite element analysis of embankments supported on geocell layer using composite model”, *Proc. of 10th International Conference on Computer Methods and Advances in Geomechanics*, IICMAG 2001, Arizona (USA).
- Rimoldi, P. and Ricciuti, A. (1994), “Design method for three dimensional geocells on slopes”, *Proc. of Fifth International Conference of Geotextiles, Geomembranes and Related Products*, Singapore, 999-1002.
- US Army Corps of Engineers (1990), “Settlement analysis”, *Engineer manual EM-1110-1-1904*, Joint Departments of the Army and Air Force, Washington, D.C.
- Wu, K.J. and Austin, D.N. (1992), “Three-dimensional polyethylene geocells for erosion control and canal linings”, *Geotext. Geomembranes*, **11**, 611-620.
- UFGS-35 73 13 (2008), “Embankment for earth dams”, *Unified Facility Guide Specifications*, US Army Corps of Engineers, Washington, D.C.